# Absolute and Convective Instabilities in Non-local Active-Dissipative Equations Arising in the Modelling of Thin Liquid Films

Dmitri TSELUIKO [1,*], Mark G. BLYTH [2], Demetrios T. PAPAGEORGIOU [3]

* Corresponding author: Tel.: +44 (0)1509 223190; Fax: +44 (0)1509 223969; Email: d.tseluiko@lboro.ac.uk
1 Department of Mathematical Sciences, Loughborough University, UK
2 School of Mathematics, University of East Anglia, UK
3 Department of Mathematics and Department of Chemical Engineering, Imperial College London, UK

**Abstract** Absolute and convective instabilities in a non-local model that arises in the analysis of thin-film flows over flat or corrugated walls in the presence of an applied electric field are discussed. Electrified liquid films arise, for example, in coating processes where liquid films are deposited onto a target surfaces with a view to producing an evenly coating layer. In practice, the target surface, or substrate, may be irregular in shape and feature corrugations or indentations. This may lead to non-uniformities in the thickness of the coating layer. Attempts to mitigate film-surface irregularities can be made using, for example, electric fields. We analyse the stability of such thin-film flows and show that if the amplitude of the wall corrugations and/or the strength of the applied electric field is increased the convectively unstable flow undergoes a transition to an absolutely unstable flow.

**Keywords:** Absolute/Convective Instability, Thin Films, Boundary Integral Methods, Non-local Equations

## 1. Introduction

Liquid-film flow down a flat or corrugated substrate has been the subject of active research in recent decades due to its numerous applications and due to its complexity. Industrial applications include for example heat and mass transfer devices and coating technologies (e.g. Weinstein and Ruschak, 2004).

When a liquid film flows down a corrugated wall, its surface deforms in response to the corrugations. On one hand, this may be a desirable feature, for example, for heat and mass transfer application (e.g. Park and Nosoko, 2003). On the other hand, in coating applications, it may be necessary to obtain a uniform coating layer and to avoid waviness of the interface.

Numerous theoretical attempts have been made to analyse film flow over topography (e.g. Tougou, 1978; Malamataris and Bontozoglou, 1999; Trifonov, 2004; Wierschem et al., 2008) and there have been numerous experimental investigations for film flows over sinusoidal and rectangular topographies (e.g. Wierschem et al., 2003; Decré and Baret, 2003; Argyriadi et al., 2006). More recent experiments of Cao et al. (2013) have uncovered novel instabilities in the form of global modes. The existence of global modes in reduced model equations has been confirmed by Tseluiko et al. (2013).

To manipulate the flow of a liquid film, an electric field may be used. Electric fields have been proposed, for example, to prevent leakage of coolant in cooling applications (e.g. Bankoff et al., 2002; Griffing et al., 2006; Kim et al., 1994), to promote micromixing (e.g. Oddy et al., 2001) and for pattern creation (e.g. Schaffer, 2000). An electric field may act either to smooth out or to promote irregularities on the film surface. For example, Tseluiko and Papageorgiou (2006) analysed the perfect-conductor film flow down and inclined plane in the presence of an applied electric field and showed that the electric field has destabilizing effect and promotes complicated interfacial dynamics. Tseluiko et al. (2008a,2008b,2009,2011) electrified film

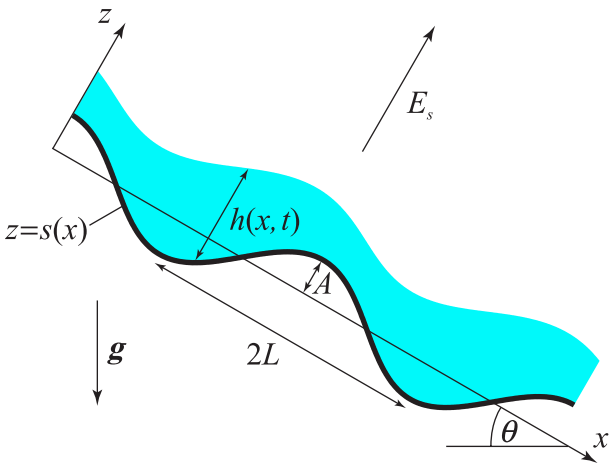


**Fig. 1.** Gravity-driven flow of a liquid film down a wavy wall in the presence of an electric field.

flow down rectangular topographies and showed, for instance, that an electric field, when applied to film flow over a downward step, can be used to eliminate the capillary ridge that develops right above the step (see Kalliadasis et al., 2000).

In the present paper, we focus on the stability analysis of non-electrified and electrified film flow down a wavy wall, and, in addition analyse the nature of instability.

The rest of the paper is organised as follows. In Section 2, we introduce the long-wave model. In Section 3, we formulate the linear stability problem. Section 4 is devoted to results. Finally, in Section 5, we present conclusions.

## 2. Model Equation

We consider gravity-driven flow of a liquid film down a wavy periodic wall which is inclined at an angle $\theta$ to the horizontal. We introduce Cartesian coordinates $(x,z)$ with the $x$-axis pointing in the direction of the flow, as shown in figure 1. We assume that the film is additionally subjected to an electric field that acts in the positive $z$-direction with strength $E_s$ sufficiently far from the film. It is assumed that the liquid film is a perfect conductor and the air above the film is a perfect dielectric. As a model, we consider the following long-wave equation (see Tseluiko and Blyth 2009):

$$h_t + q_x = 0, \tag{1}$$

where $h(x,t)$ denotes the film thickness $q(x,t)$ is the flow rate given by

$$q = \frac{2}{3}h^3 + \frac{8R}{15}h^6 h_x - \frac{2\cot\theta}{3}h^3(h+s)_x + \frac{1}{3C}h^3(h+s)_{xxx} + \frac{2W}{3}h^3\mathcal{H}[h_{xx}+s_{xx}], \tag{2}$$

where $s(x)$ is the topography shape. The last term represents the effect of the imposed electric field and is derived by solving the harmonic problem for the electric potential in the air (see Tseluiko and Papageorgiou 2006), and the symbol $\mathcal{H}$ denotes the Hilbert transform operator

$$\mathcal{H}[f](x) = \frac{1}{\pi}PV\int_{-\infty}^{\infty}\frac{f(y)}{y-x}\mathrm{d}y, \tag{3}$$

where $PV$ denotes the principal value of the integral. The dimensionless parameters are the Reynolds number $R$, the capillary number $C$ and the electric Weber number $W$ that are defined by

$$R = \frac{\rho h_s U_s}{\mu}, \quad C = \frac{\mu U_s}{\gamma}, \quad W = \frac{\varepsilon E_s^2 h_s}{2\mu U_s}, \tag{4}$$

where $\rho$ is the liquid film density, $\mu$ is the dynamics viscosity, $\gamma$ is the surface tension coefficient and $\varepsilon$ is the air permittivity. Also, $h_s$ is the typical film thickness and $U_s = \rho g h_s^2 \sin\theta / 2\mu$ is the surface speed of a Nusselt flat film of thickness $h_s$ flowing down a flat plate at an angle $\theta$ to the horizontal. Note that the dimensionless parameters are defined based on the Nusselt surface speed but not on the mean speed as is also often done in the literature. In experiments, typically the flow rate $Q$ is imposed, and in such a case the Nusselt film thickness and the surface velocity are given by

$$h_s = \left(\frac{3\mu Q}{\rho g \sin\theta}\right)^{1/3}, \quad U_s = \frac{3Q}{2h_s}. \tag{5}$$

It will be convenient to note that $C = (R^{2/3}\sin^{1/3}\theta)/(2^{1/3}K)$, where

$$K = \frac{\gamma\rho^{1/3}}{g^{1/3}\mu^{4/3}} \tag{7}$$

is the Kapitza number, which depends only on the physical properties of the liquid.

## 3. Steady-state Solutions

We will consider the topography of a sinusoidal shape given by

$$s(x) = A\cos(\pi x / L), \tag{8}$$

where $A$ is the dimensionless amplitude and $L$ is the dimensionless half-period of the wall. A steady-state solution $h_0(x)$ of half-period $L_c = nL$ satisfies the equation

$$\begin{aligned} q_0 = {} & \frac{2}{3}h_0^3 + \frac{8R}{15}h_0^6 h_{0x} - \frac{2\cot\theta}{3}h_0^3(h_0+s)_x \\ & + \frac{1}{3C}h_0^3(h_0+s)_{xxx} + \frac{2W}{3}h_0^3\mathcal{H}[h_{0xx}+s_{xx}], \end{aligned} \tag{9}$$

where $q_0$ is a constant. We consider two scenarios. In the first scenario, we fix the volume of fluid in one period, in which case we impose the integral condition $(1/2L)\int_{-L_c}^{L_c} h_0\,\mathrm{d}x = 1$. Alternatively, this can be thought of as fixing the average film thickness. In the second scenario, we instead fix the flow rate in the film, and in particular we set $q_0 = 2/3$, where $q_0$ is obtained by replacing $h$ by $h_0$ in (2). Note that for a flat wall taking $q_0 = 2/3$ corresponds to a flat Nusselt film of unit dimensionless thickness. We obtain steady-state solutions using a spectral numerical scheme based on representing spatial derivatives using Fast Fourier Transform algorithm and utilizing Newton iterations to obtain solutions from initial guesses.

## 4. Linear Stability Analysis

Our primary concern will be to analyse the linear stability of steady state solutions to the model equation (1). To this end, we next derive a linearised form of this equation on the assumption that any deviations from a given steady state solution are only small. Suppose that $h_0(x)$ represents a steady-state solution. We write $h = h_0(x) + \eta(x,t)$, where $\eta$ is a small perturbation. Substituting this ansatz into (1) and linearising, we obtain

$$\eta_t = \mathcal{L}\eta, \tag{10}$$

where $\mathcal{L}$ is the linear integro-differential operator with periodic coefficients,

$$\mathcal{L}\eta = -(b_0\eta + b_1\eta_x + b_2\mathcal{H}[\eta_{xx}] + b_3\eta_{xxx})_x, \tag{11}$$

where

$$\begin{aligned} b_0 = {} & 2h_0^2 + \frac{16R}{5}h_0^5 h_{0x} - (2\cot\theta)h_0^2(h_0+s)_{xxx} \\ & + 2Wh_0^2\mathcal{H}[h_{0xx}+s_{xx}], \end{aligned} \tag{12}$$

$$b_1 = \frac{8R}{15}h_0^6 - \frac{2\cot\theta}{3}h_0^3, \tag{13}$$

$$b_2 = \frac{2W}{3}h_0^3, \tag{14}$$

$$b_3 = \frac{1}{3C}h_0^3. \tag{15}$$

Although in our analysis we assume that both the wall topography $s(x)$ and the steady state solution $h_0(x)$ are periodic functions, it will be crucial to our discussion to realise that the perturbation $\eta(x,t)$ is not restricted to the class of spatially-periodic functions. The flow stability depends on the spectrum of the operator $\mathcal{L}$, which is denoted by $\sigma(\mathcal{L})$. If part of the spectrum belongs to the right half of the complex plane, the solution is linearly unstable, and perturbations will grow in time. Otherwise, if the spectrum belongs to the left half-plane, the solution is linearly unstable.

In addition, if the electric-field term is absent, the governing equation is local and the nature of instability can be analysed. A convenient and elegant way to do this is by utilising the exponentially-weighted-spaces approach (e.g. Sandstede and Scheel, 2000). We define space $L_a^2$ with the inner product

$$L_a^2 = \{f : \mathrm{e}^{ax} f \in L^2\}, \tag{16}$$

where $a$ is a real constant. It can be shown that studying the spectrum of $\mathcal{L}$ in $L_a^2$ is equivalent to studying the spectrum of the following modified operator in the usual $L^2$-space:

$$\begin{aligned} \mathcal{L}_a f = {} & \mathrm{e}^{ax}\mathcal{L}(\mathrm{e}^{-ax} f) \\ = {} & [b_3(f_{xxx} - 3af_{xx} + 3a^2 f_x - a^3 f)]_x \\ & - ab_3(f_{xxx} - 3af_{xx} + 3a^2 f_x - a^3 f) \\ & + [b_1(f_x - af)]_x - b_1(f_x - af) \\ & + (b_0 f)_x - ab_0 f, \end{aligned} \tag{17}$$

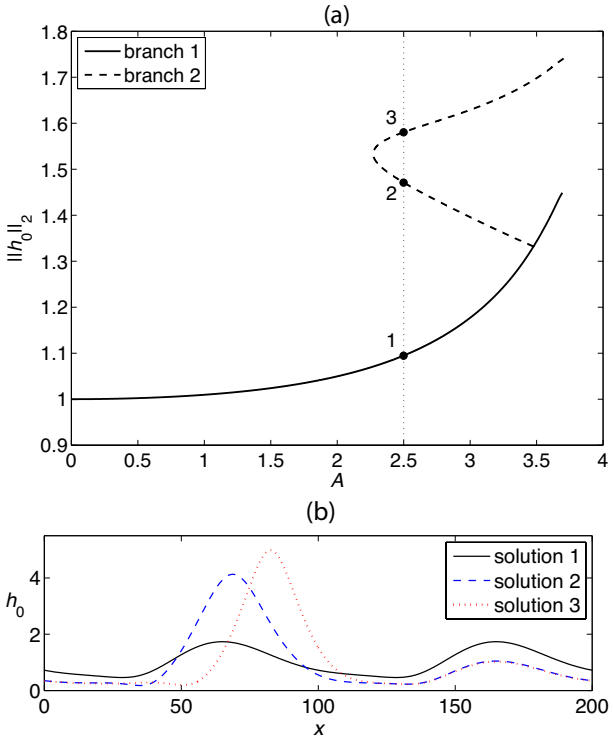


**Fig. 2.** (a) $L^2$-norm of steady-state solutions in dependence on the wall amplitude $A$ when the wall half-period is $L = 50$. The solid line shows the branch of $2L$-periodic solutions. The dashed line shows the branch of subharmonic solutions of period $4L$. Labels 1, 2, and 3 indicate solutions for $A = 2.5$ that are shown in panel (b).

where $b_0$, $b_1$, and $b_3$ are defined in (11), (12), and (14), respectively. If for some $a$ it is possible to shift the spectrum of the modified operator to the left half-plane, then the solution is convectively unstable. Otherwise, the solution is absolutely unstable and propagates both upstream and downstream. The point spectrum of this operator is empty (see, for example, Sandstede, 2002, §3.4.2). To compute the essential spectrum, we use the Floquet-Bloch theory and obtain that the spectrum of $\mathcal{L}_a$ is given by

$$\sigma(\mathcal{L}_a) = \bigcup_{k\in[-\pi/(2L),\pi/(2L)]} \sigma(\mathcal{L}_{a,k}), \qquad (18)$$

where

$$\mathcal{L}_{a,k}[f] = \mathrm{e}^{(a-\mathrm{i}k)x}\mathcal{L}[\mathrm{e}^{-(a-\mathrm{i}k)x}f] = \mathcal{L}_{a-\mathrm{i}k}[f]. \qquad (19)$$

It should be noted that for the non-local model with the electric-field term the exponentially-weighted-spaces approach is not applicable since the Hilbert transform term is only defined on the Schwartz class of tempered distributions, which does not include exponentially growing functions. Therefore, in such a case, we analyse the nature of instability numerically (as will be explained below).

## 5. Results

In this section, we study the effect of wall corrugations on the stability of film flow using the methods described above. Our aim is to compute the steady solution for a given set of parameter values and then to calculate the essential spectrum of $\mathcal{L}_a$ to determine the stability characteristics of the steady flow. To provide a focus for our discussion, we will describe results for a specific fluid, namely, we will consider water, for which the Kapitza number is $K \approx 3364.5$. Also, we will fix the wall inclination angle to be $\pi/4$.

### 5.1. Flows with no electric field

Figure 2(a) shows the bifurcation diagram for steady solutions for flow of water down a wavy wall of dimensionless half-period $L = 50$. The wall amplitude $A$ is chosen as the control parameter and the $L^2$-norm $\|h_0\|_2$ is chosen as the measure of the solutions. The primary branch of solutions is shown by a solid line. It is interesting to note that there exist subharmonic solutions which have the period twice that of the wall, and which bifurcate from the primary branch at $A = A_b = 3.4769$ (see Tseluiko et al., 2013 for more details). The branch of subharmonic solutions is shown by a dotted line in Fig. 2(a). It can be observed that this branch has a turning point. Both the primary and the subharmonic branch terminate at the points where the minima of the film thicknesses reach zero. The solution profiles corresponding to labeled points 1, 2 and 3 are shown in Fig. 2(b).

The stability computations for the primary branch show that the solutions become unstable at the wall amplitude $A = 3.4765$ that is less than the value $A_b$ at which the subharmonic branch bifurcates. Before the instability onset, a gap in the spectrum appears, i.e. the spectrum consists of an isolated loop passing through zero with the

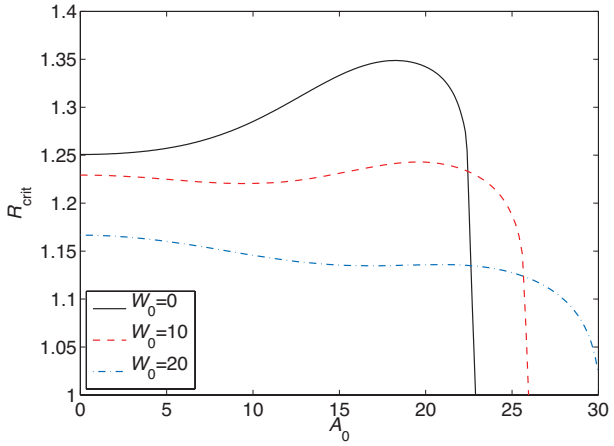


**Fig. 3.** Dependence of the critical Reynolds number on the wall amplitude $A_0$ for water ($K$ = 3364.5) when $\theta = \pi/4$ and $L_0$ = 150 for $W_0$ =0, 10 and 20 (solid, dashed, and dash-dotted lines, respectively). The wall shape is sinusoidal.

remaining part of the spectrum being located to the left of this loop. Beyond the instability threshold, part of the spectrum moves to the right half-plane. For even larger values of $A$, the whole loop belongs to the right half-plane. Also, we find that for $3.4765 < A < 3.4767$ the instability is convective, but it becomes absolute for larger values of $A$, i.e. for larger values of the wall amplitude there is always part of the spectrum of the modified operator $\mathcal{L}_a$ that belongs to the right half of the complex plane. As far as the subharmonic branch is concerned, we find that its solutions are absolutely unstable.

It should be noted that we find qualitatively similar results for the case of the fixed flow rate, namely, we find that there can exist branches of subharmonic solutions and the instability can change from convective to absolute. The main difference is that for the fixed flow rate case the branches do not terminate.

### 5.2. Electrified flow

It can be easily verified that the electric field is always linearly destabilising for the case of a flat wall. To analyse stability of electrified flow over a wavy wall, we compute the essential spectrum of the operator $\mathcal{L}$ given by (11) by again invoking the Floquet-Bloch theory. Since we would ultimately wish to compare our results with experiments, it will be convenient to note that the dimensionless wall amplitude and period can be written as

$$A = \frac{A_0 \sin^{1/3}\theta}{R^{1/3}}, \quad L = \frac{L_0 \sin^{1/3}\theta}{R^{1/3}}, \tag{20}$$

where

$$A_0 = \frac{\tilde{A}\rho^{2/3} g^{1/3}}{2^{1/3}\mu^{2/3}}, \quad L_0 = \frac{\tilde{L}\rho^{2/3} g^{1/3}}{2^{1/3}\mu^{2/3}}, \tag{21}$$

and $\tilde{A}$ and $\tilde{L}$ denote the dimensional wall amplitude and half-period, respectively. We note that $A_0$ and $L_0$ are independent of the Reynolds number and the inclination angle. We therefore choose to work with these parameters, when discussing the dependence of the critical Reynolds number on the wall amplitude. This permits us to vary the flow parameters but still refer to the same fluid and the same wall geometry. In addition, we note that

$$W = \frac{W_0}{R^{1/3}\sin^{2/3}\theta}, \tag{22}$$

where

$$W_0 = \frac{\varepsilon E_s^2}{2^{1/3}\rho^{1/3} g^{2/3}\mu^{2/3}}. \tag{23}$$

The parameter $W_0$ depends only on the physical properties of the liquid, the permittivity of the surrounding air and the strength of the applied electric field.

Figure 3 shows the dependence of the critical Reynolds number on the dimensionless wall amplitude, $A_0$, for water (when $K$ = 3364.5) for $L$ = 150. The results were obtained for the fixed volume case. The solid, dashed and dot-dashed lines correspond to $W_0$ = 0, 10, and 20, respectively. It can be observed that initially, for sufficiently small values of the wall amplitude, the electric field is destabilising in the sense that the dashed line corresponding to $W_0$ = 10 lies below the solid one corresponding to $W_0$ = 0, and the dot-dashed line corresponding to $W_0$ = 20 lies below the dashed one. Also, without the electric field, the critical Reynolds number initially increases with the wall amplitude, whereas in the presence of the electric field, the critical Reynolds number may initially decrease, then

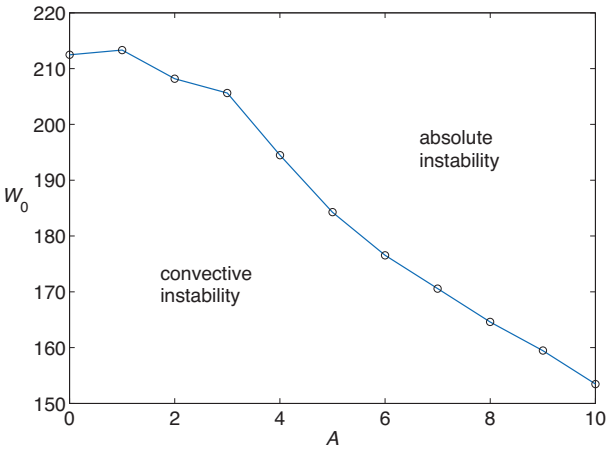


**Fig. 4**. Absolute and convective instability for electrified flow of water ($K$ = 3364.5) at $R$ = (5/4) cot $\theta$ down a wall of dimensionless period $L$ = 100 inclined at an angle $\theta = \pi/4$. The results are shown in the $(A,W_0)$-plane. The region above the solid line corresponds to absolutely unstable flows. The region below the solid line corresponds to convectively unstable flows.

increase and then decrease again. We also find that the electric field may have a stabilising effect on the flow in the sense that for some values of the wall amplitude and the Reynolds number, the non-electrified flow is unstable, but the corresponding electrified flow is stable. Indeed, it can be seen that beyond some wall amplitude the dashed and the dot-dashed lines lie above the solid one.

Finally, we discuss absolute and convective instabilities of electrified film flow. As was noted above, the exponentially-weighted-spaces approach is not applicable for the non-local equation modelling such a flow. We therefore analyse this numerically. We choose $\theta=\pi/4$ and set the Reynolds number at its critical value for a flat wall, namely $R = (5/4)\cot\theta = 5/4$. We fix $L$ = 100 and compute steady solutions for various values of the $A$ and $W_0$. We also assume that the flow rate is fixed, $q_0 = 2/3$. The linearised equation (10) is solved numerically using FFTs for spatial derivatives with the initial condition $\eta(x,0) = \delta(x + L)$. (Numerically, this is achieved by requiring that the FFT coefficients of the initial conditions are all equal to 1.) The instability is concluded to be convective if the solution approaches zero in time at a fixed $x$ location; otherwise, the instability is absolute. The results are shown in Fig. 4. For sufficiently small wall amplitudes, a stronger electric field (as compared to the flat wall case) is required to switch the dynamics from the convectively unstable regime to the absolutely unstable regime. For sufficiently large values of the wall amplitude, the critical electric field parameter $W_0$ which marks the division between absolute from convective instability is a monotonically decaying function of the wall amplitude $A$.

## 6 Conclusions

We have analysed gravity-driven liquid film flow down inclined corrugated walls in the presence of an electric field. We used a Benney-type long-wave model equation. We computed various solution branches and demonstrated that there exist subharmonic and quasi-periodic solutions. We analysed the stability of the solutions and found that the topography can stabilise or destabilise the flow depending on the wall period and amplitude. In addition we found that the flow can undergo the transition to absolute instability, in agreement with recent experimental results of Cao et al. (2012). We compared our results with time-dependent simulations and found good agreement. In addition, we found that the effect of the imposed electric field depends on the wall amplitude. For small wall amplitudes, we found that the electric field has a destabilising effect on the flow. However, if the wall amplitude in sufficiently large, we find that the electric field can have a stabilising effect on the flow. We also found that a convectively unstable flow down a wavy wall can undergo the transition to absolute instability, if the strength of the applied electric field becomes sufficiently large.

## Acknowledgements

We acknowledge financial support from the EPSRC under grant EP/K041134/1. The work of DT and MGB was partly supported by the London Mathematical Society under the grant 41114. The work of DT was additionally supported by the EPSRC under grant EP/J001740/1.

## References

Argyriadi, K., Vlachogiannis, M., Bontozoglou, V., 2006. Experimental study of inclined film flow along periodic corrugations: The effect of wall steepness. Phys. Fluids 18, 012102.

Bankoff, S.G., Griffing, E.M., Schluter, R.A., 2002. Use of an electric field in an electrostatic liquid film radiator. Ann. N.Y. Acad. Sci. 974, 1–9.

Cao, Z., Vlachogiannis, M., Bontozoglou, V., 2013. Experimental evidence for a short-wave global mode in film flow along periodic corrugations. J. Fluid Mech. 718, 304–320.

Decré, M.M.J., Baret, J.C., 2003. Gravity-driven flows of viscous liquids over two-dimensional topographies. J. Fluid Mech. 487, 147–166.

Griffing, E.M., Bankoff, S.G., Miksis, M.J., Schluter, R.A., 2006. Electrohydrodynamics of thin flowing films. J. Fluids Eng. 128, 276–283.

Kalliadasis, S., Bielarz, C., Homsy, G.M., 2000. Steady free-surface thin film flows over topography. Phys. Fluids 12, 1889–1898.

Kim, H., Miksis, M.J., Bankoff, S.G., 1994. The cylindrical electrostatic liquid film radiator for heat rejection in space. J. Heat Transfer 116, 986-992.

Malamataris, N.A., Bontozoglou, V., 1999. Computer aided analysis of viscous film flow along an inclined wavy wall. J. Comput. Phys. 154, 372–392.

Oddy, H., Santiago, J.G., Mikkelsen, J.C., 2001. Electrokinetic instability micromixing," Anal. Chem. 73, 5822–5832.

Park, C.D., Nosoko, T., 2009. Three-dimensional wave dynamics on a falling film and associated mass transfer. AIChE J. 49, 2715–2727.

Sandstede, B., 2002. Stability of travelling waves pp. 983–1055, In: B. Fiedler, ed. Handbook of Dynamical Systems II, North-Holland.

Sandstede, B., Scheel, A., 2000. Absolute and convective instabilities of waves on unbounded domains. Physica D 145, 233–277.

Schaffer, E., Thurn-Albrecht, T., Russel, T.P., Steiner, U., 2000. Electrically induced structure formation and pattern transfer. Nature 403, 874–877.

Tougou, H., 1978. Long waves on a film flow of a viscous fluid down an inclined uneven wall. J. Phys. Soc. Japan 44, 1014–1019.

Trifonov, Yu.Ya., 2004, Viscous film flow down corrugated surfaces. J. Appl. Mech. Tech. Phys. 45, 389–400.

Tseluiko, D., Blyth, M.G., 2009. Effect of inertia on electrified film flow over a wavy wall. J. Eng. Math. 65, 229–242.

Tseluiko, D., Blyth, M.G., Papageorgiou, D.T., 2013. Stability of film flow over inclined topography based on a long-wave nonlinear model. J. Fluid Mech. 729, 638–671.

Tseluiko, D., Blyth, M.G., Papageorgiou, D.T., Vanden-Broeck, J-M., 2008a. Effect of an electric field on film flow down a corrugated wall at zero Reynolds number. Phys. Fluids 20, 042103.

Tseluiko, D., Blyth, M.G., Papageorgiou, D.T., Vanden-Broeck, J.-M., 2008b. Electrified viscous thin film flow over topography. J. Fluid Mech. 597, 449.

Tseluiko, D., Blyth, M.G., Papageorgiou, D.T., Vanden-Broeck, J-M., 2009. Viscous electrified film flow over step topography. SIAM J. Appl. Math. 70, 845–865.

Tseluiko, D., Blyth, M.G., Papageorgiou, D.T., Vanden-Broeck, J-M., 2011. Electrified film flow over step topography at zero Reynolds number: an analytical and computational study. J. Eng. Math. 69, 169–183.

Tseluiko,, D., Papageorgiou, D.T., 2006. Wave evolution on electrified falling films. J. Fluid Mech. 556, 361–386.

Weinstein, S.J., Ruschak, K.J., 2004. Coating flows. Annu. Rev. Fluid Mech. 36, 29–53.

Wierschem, A., Bontozoglou, V., Heining, C., Uecker, H., Aksel, N. 2008. Linear resonance in viscous films on inclined wavy planes. Int. J. Multiphase Flow 34, 580–589.

Wierschem, A., Scholle, M., Aksel, N. 2003. Vortices in film flow over strongly undulated bottom profiles at low Reynolds numbers. Phys. Fluids 15, 426–435.